ChemComm

COMMUNICATION

View Article Online
View Journal | View Issue

Cite this: *Chem. Commun.*, 2014, **50**, 2052

Received 8th October 2013,
Accepted 20th December 2013

DOI: 10.1039/c3cc47719c

www.rsc.org/chemcomm

One step preparation of a high performance Ge–C nanocomposite anode for lithium ion batteries by tandem plasma reactions†

Wei Li, Jie Zheng,* Tiankai Chen, Teng Wang, Xiaojuan Wang and Xingguo Li*

We employ a tandem plasma reaction method to prepare ultrafine Ge nanoparticles embedded in a carbon matrix in one step. The obtained Ge–C composite exhibits very high lithium storage capacity (980 mA h g^{-1}) and excellent cycling performance (less than 2% capacity loss in 100 cycles).

The quick development of modern society requires more demanding energy storage systems. Lithium-ion batteries (LIBs), owing to their high energy density and good cycle stability, may meet this requirement. LIBs have been widely applied in portable electronic devices and are also very promising for electric vehicles. Many studies have been devoted to develop high performance anode materials for LIBs, such as Si (4200 mA h g^{-1})[1] and Ge (1600 mA h g^{-1})[2] to replace the conventional graphite (372 mA h g^{-1})[3] anode. However, the capacities of these anodes fade rapidly with the charging and discharging processes as they suffer from extremely large volume changes.[4] Numerous efforts have been devoted to improve the cycling performance of these anode materials, including using nanoparticles or nanowires,[5] porous structure,[6] carbon coating[7] and alloying with metals.[8] The essential point to improve the electrode performance is reducing the particle size and releasing the stress caused by volume expansion. Ge has received less attention than Si due to its lower capacity. However, the Li diffusion rate is faster in Ge than in Si,[9] which means that Ge may be an attractive electrode material for high-charging-rate LIBs. Nanostructures of Ge have been widely reported, showing promising capacity and cycling stability.[10] Among these morphologies, nanowires exhibit impressive cycling performance and high stable capacity.[11] Meanwhile, the nanowire was significantly thickened and elongated after lithiation according to *in situ* TEM observations in Liu's research.[12] This result inspires efforts to further stabilize the structure by reinforcing the walls of nanowires. However, there is a potential problem in long time use of the LIBs with this nanowire structure anode. Once the walls of the nanowires break off, the active materials would "outflow" from the nanowires, which may cause a ripple effect, resulting in quick capacity loss. The most desirable structure should be 0D nanoparticles. By coating with carbon or embedding in the carbon matrix, the nanoparticles can be protected all-around.[13] The conventional ways to prepare carbon coated Ge nanoparticles are mainly based on the polymerization–carbonization process.[10c,14] Usually, organic precursors are polymerized on Ge nanoparticles in one or two steps. Then with high temperature carbonization treatment, a carbon layer coated on the Ge surface is formed. However, this two or more step method is not only inconvenient, but also energy inefficient as the high temperature treatment is required.

Here, we present a tandem plasma reaction approach to prepare ultrafine Ge–C nanostructure. In this method, the generation of the Ge and C components is independently controlled in separated plasma zones, enabling variation of the composition and structure of the Ge–C composite. Ultrafine Ge nanoparticles embedded in the carbon matrix are prepared. This structure shows great improvement in the cycling stability of the active material. The Ge–C composite exhibits a capacity of nearly 980 mA h g^{-1} after 100 cycles under a current density of 2000 mA g^{-1}, with a total capacity loss of less than 2%. This structure may be used as high performance anode material for LIBs. Besides, this tandem plasma reaction method has the potential to extend to the Si–C system, which is more difficult to prepare using the conventional method and may achieve much higher capacity.

Compared to chemical reactions activated by thermal energy, plasma enhanced chemical reactions are advantageous in terms of higher efficiency, lower reaction temperature and the opportunity to obtain novel nanostructures.[15] Considering binary nanocomposites, an appropriate reactor design will further improve the versatility during the preparation process. As shown in Fig. 1, the Ge–C composite samples are deposited in a home-designed tandem plasma reactor consisting of a magnetron sputtering source and an inductive coil.[16] Ge particles are generated by magnetron sputtering of a high purity Ge target, and are coated with carbon in the ICP zone by decomposition of CH_4. Such a configuration

---

Beijing National Laboratory for Molecular Sciences (BNLMS), The State Key Laboratory of Rare Earth Materials Chemistry and Application, College of Chemistry and Molecular Engineering, Peking University, Beijing, 100871, China. E-mail: xgli@pku.edu.cn; Tel: +86 10 6276 5930

† Electronic supplementary information (ESI) available: Details of preparation and characterization. See DOI: 10.1039/c3cc47719c

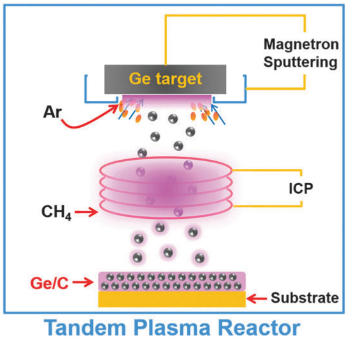

Fig. 1 Schematic illustration of the tandem plasma reactor and the preparation process of the Ge–C composites.

affords spatially separated zones for the generation of the two components, which allow large freedom in composition/particle size control. Compared to co-sputtering with two magnetron sources, the tandem plasma reactor allows using gaseous hydrocarbon precursors instead of a solid target, which will give a more homogeneous plasma zone for carbon coating.[17] The products are directly deposited on copper foils and silicon substrates at room temperature. And the obtained products are uniform films with sufficient adhesion to the substrates, which can be directly used as the electrodes without further treatment.

The EDS results (ESI,† Fig. S1) suggest that the composite contains both Ge and C, apart from the Cu substrate. Quantitative analysis indicates that the Ge–C composite is composed of 12.4 wt% C and 87.6 wt% Ge, which is also determined by the XPS results (Fig. S2, ESI†). The TEM results demonstrate the structure of pure Ge (Fig. 2a) and the Ge–C composite (Fig. 2c). It is clearly observed that the pure Ge film is composed of compactly packed Ge nanoparticles with an average diameter of 15 nm. From the selected area electron diffraction (SAED) pattern, diffraction rings can be distinguished while the fringes are blurred (Fig. 2b), which may be attributed to the very small crystallite size of the Ge particles. The Ge–C composite is composed of Ge nanoparticles of around 30 nm according to the TEM image (Fig. 2c), which is larger than that of pure Ge. However, the HRTEM image (Fig. 2e) indicates that the Ge–C composites have secondary structure, consisting of much smaller Ge particles in amorphous carbon. The ultrafine Ge nanoparticles are less than 5 nm in diameter. The carbon matrix simply prevents the Ge nanoparticles from contacting and aggregating. Besides, it also provides a buffer for the volume change during charge and discharge. Moreover, the SAED pattern of the Ge–C composite (Fig. 2d) shows that the Ge nanoparticles are not as well crystallized as pure Ge, which is in good agreement with the HRTEM results. The above information implies that the Ge–C composite is composed of ultrafine Ge nanoparticles embedded in the amorphous carbon matrix and the pure Ge sample is composed of well-defined nanoparticles.

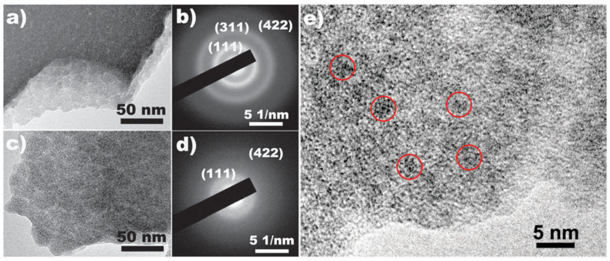

Fig. 2 (a, b) TEM image and SAED pattern of the pure Ge; (c, d) TEM image and SAED pattern of the Ge–C composite; (e) HRTEM image of the Ge–C composite. The red circles designate the ultrafine Ge nanoparticles in the carbon matrix.

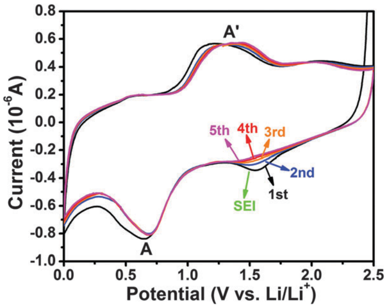

Fig. 3 A typical cyclic voltammograph of Ge–C composite electrode.

Fig. 3 shows a typical CV graph for the Ge–C samples directly deposited on copper foils. The pair peaks A–A′ in the voltage range of 0.6–1.2 V *vs.* Li/Li$^+$ are associated with the electrochemical reaction between Li and Ge (eqn (1)).[18]

$$x\text{Li} + \text{Ge} \rightarrow \text{Li}_x\text{Ge} \tag{1}$$

The first cycle shows some irreversible capacity which is attributed to the formation of the solid electrolyte interface (SEI) in the voltage range of 1.6 V. And the irreversible peak gradually disappears along with the cycling in the subsequent cycles. The CV curves of the following cycles are almost overlapped, indicating that the Ge–C composites have good cycling stability during charge–discharge.

The assembled half cells were tested by galvanostatic charge–discharge cycling. Fig. 4a and b show the voltage profiles of the 1st, 2nd, 5th and 100th cycles at a current density of 2000 mA g^{-1} in a voltage window of 0.005–1.5 V at room temperature for pure Ge and the Ge–C composite, respectively. The pure Ge shows a

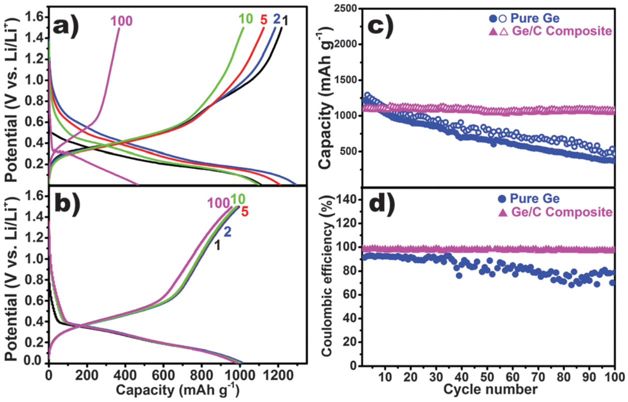

Fig. 4 Charge and discharge curves of the pure Ge (a) and Ge–C composite (b) electrode, respectively. (c) The cycling performance of pure Ge and Ge–C composite at a charge and discharge rate of 2000 mA g^{-1}, hollow symbols: discharge, solid symbols: charge. (d) Coulombic efficiency of the pure Ge and Ge–C composite.

high capacity of nearly 1200 mA h g^{-1} in the first cycle. However, it declines along with every cycle, which may be caused by the fragmentation of the anode in the cycling, and the formation of the SEI layer on the fragmented anode surface.[19] The Ge–C composite shows a high capacity of nearly 1000 mA h g^{-1} in the first cycle. Though it is lower compared to the first cycle of pure Ge, it retains near 98% capacity in the next 100 cycles, which means almost no fragments and few SEI layers were formed.

A key parameter measuring the electrode performance of the Ge–C composites is the reversible capacity. The charge and discharge curves of pure Ge and Ge–C binary composites are shown in Fig. 4a and b up to 100 cycles. It is clearly observed that the pure Ge film exhibits a quick capacity loss in the first 10 cycles. And after 100 cycles, only a capacity of 380 mA h g^{-1} is retained, which is 68% capacity loss compared to the first cycle. In contrast, the Ge–C composite shows great improvement in the cycling performance. The Ge–C composite exhibits a capacity of 1000 mA h g^{-1} in the first cycle. Though it is lower than that of pure Ge, the capacity exhibits no more than 2% capacity loss up to 100 cycles, showing excellent stability. Since carbon is known to have a low but very stable capacity (372 mA h g^{-1} for graphite), the excellent cycling stability indicates that the Ge particles are effectively stabilized during the charge–discharge processes. This capacity stability is comparable with the state-of-the-art results.[10*a*,14*b*,20] It is also worthwhile to note that the coulombic efficiency of the Ge–C composite remains around 98% in all cycles, which is more stable and much higher than that of pure Ge, as shown in Fig. 4d.

The excellent capacity retention property is attributed to the structure of the Ge–C composite. The main reason for the capacity decay of the pure Ge is the severe volume change during the charge–discharge processes. The smaller particle size of the active material is beneficial to the cycling stability since it reduces the absolute volume change. The carbon coating surrounding the Ge particles provides a further buffering effect. Moreover, it also prevents the Ge nanoparticles from aggregating during charge and discharge. It is worth noting that the excellent stability is obtained without much loss of the capacity, since the carbon fraction is only 12.4 wt%. The notable stabilization effect is attributed to the homogeneous mixing of the nascent Ge clusters with the carbon precursor in the ICP zone, as evidenced by the homogeneous distribution of the ultrafine Ge particles of only several nanometres in the carbon matrix (Fig. 2e). Such homogeneous carbon coating is very difficult to achieve by surface modification of post-synthesized Ge particles.

Generally, the Ge–C composite exhibits excellent cycling performance with a stable capacity of 980 mA h g^{-1} and splendid coulombic efficiency. This ultrafine Ge nanoparticle embedded in the carbon matrix structure shows great potential to be used as a high performance anode for LIBs.

In conclusion, Ge–C composites with ultrafine Ge nanoparticles embedded in the carbon matrix are prepared by a tandem plasma reaction method. In this method, the generation of the Ge and C components is independently controlled in separated plasma zones, enabling a great opportunity to coat Ge nanoparticles homogeneously with carbon and prevent the Ge nanoparticles from aggregating. This well-tailored structure results in high reversible capacity. This performance–structure correlation will provide useful insights into the design of carbon based composite anode materials for LIBs. The tandem plasma reaction method and the principles of composition control can also be readily extended to a large variety of metal–carbon binary composites.

The authors acknowledge MOST of China (No. 2010CB631301 and 2012CBA01207) and NSFC (No. 20821091, U1201241, 11375020 and 21321001).

Notes and references

1 B. A. Boukamp, G. C. Lesh and R. A. Huggins, *J. Electrochem. Soc.*, 1981, **128**, 725.
2 J. Sangster and A. D. Pelton, *J. Phase Equilib.*, 1997, **18**, 289.
3 S. Megahed and B. Scrosati, *J. Power Sources*, 1994, **51**, 79.
4 M. Winter, J. O. Besenhard, M. E. Spahr and P. Novak, *Adv. Mater.*, 1998, **10**, 725.
5 (*a*) T. Song, H. Cheng, H. Choi, J. H. Lee, H. Han, D. H. Lee, D. S. Yoo, M. S. Kwon, J. M. Choi, S. G. Doo, H. Chang, J. Xiao, Y. Huang, W. I. Park, Y. C. Chung, H. Kim, J. A. Rogers and U. Paik, *ACS Nano*, 2012, **6**, 303; (*b*) J. R. Szczech and S. Jin, *Energy Environ. Sci.*, 2011, **4**, 56; (*c*) Y. D. Ko, J. G. Kang, G. H. Lee, J. G. Park, K. S. Park, Y. H. Jin and D. W. Kim, *Nanoscale*, 2011, **3**, 3371.
6 (*a*) N. G. Rudawski, B. R. Yates, M. R. Holzworth, K. S. Jones, R. G. Elliman and A. A. Volinsky, *J. Power Sources*, 2013, **223**, 336; (*b*) J. Guo, A. Sun and C. Wang, *Electrochem. Commun.*, 2010, **12**, 981; (*c*) L. Shen, X. Guo, X. Fang, Z. Wang and L. Chen, *J. Power Sources*, 2012, **213**, 229.
7 (*a*) X. Q. Yang, J. McBreen, W. S. Yoon, M. Yoshio, H. Wang, K. Fukuda and T. Umeno, *Electrochem. Commun.*, 2002, **4**, 893; (*b*) N. Dimov, S. Kugino and M. Yoshio, *Electrochim. Acta*, 2003, **48**, 1579.
8 (*a*) H. Li, Z. X. Wang, L. Q. Chen and X. J. Huang, *Adv. Mater.*, 2009, **21**, 4593; (*b*) C. M. Hwang and J. W. Park, *Electrochim. Acta*, 2011, **56**, 6737.
9 (*a*) C. S. Fuller and J. C. Severiens, *Phys. Rev.*, 1954, **96**, 21; (*b*) J. Graetz, C. C. Ahn, R. Yazami and B. Fultz, *J. Electrochem. Soc.*, 2004, **151**, A698.
10 (*a*) J. Gu, S. M. Collins, A. I. Carim, X. Hao, B. M. Bartlett and S. Maldonado, *Nano Lett.*, 2012, **12**, 4617; (*b*) Y. Hwa, C. M. Park, S. Yoon and H. J. Sohn, *Electrochim. Acta*, 2010, **55**, 3324; (*c*) M. G. Kim and J. Cho, *J. Electrochem. Soc.*, 2009, **156**, A277.
11 (*a*) M. H. Seo, M. Park, K. T. Lee, K. Kim, J. Kim and J. Cho, *Energy Environ. Sci.*, 2011, **4**, 425; (*b*) C. K. Chan, X. F. Zhang and Y. Cui, *Nano Lett.*, 2008, **8**, 307.
12 X. H. Liu, S. Huang, S. T. Picraux, J. Li, T. Zhu and J. Y. Huang, *Nano Lett.*, 2011, **11**, 3991.
13 G. Jo, I. Choi, H. Ahn and M. J. Park, *Chem. Commun.*, 2012, **48**, 3987.
14 (*a*) H. Lee, H. Kim, S. G. Doo and J. Cho, *J. Electrochem. Soc.*, 2007, **154**, A343; (*b*) G. Cui, L. Gu, L. Zhi, N. Kaskhedikar, P. A. van Aken, K. Müllen and J. Maier, *Adv. Mater.*, 2008, **20**, 3079.
15 J. Zheng, B. Sun, R. Yang, X. B. Song, X. G. Li and Y. K. Pu, *J. Phys. Chem. B*, 2008, **112**, 12748.
16 W. Li, R. Yang, X. J. Wang, T. Wang, J. Zheng and X. G. Li, *J. Power Sources*, 2013, **221**, 242.
17 K. Ostrikov, E. C. Neyts and M. Meyyappan, *Adv. Phys.*, 2013, **62**, 113.
18 M. K. Y. Chan, B. R. Lone, A. A. Gewirth and J. P. Greeley, *J. Phys. Chem. Lett.*, 2011, **2**, 3092.
19 J. T. Li, S. R. Chen, F. S. Ke, G. Z. Wei, L. Huang and S. G. Sun, *J. Electroanal. Chem.*, 2010, **649**, 171.
20 D. J. Xue, S. Xin, Y. Yan, K. C. Jiang, Y. X. Yin, Y. G. Guo and L. J. Wan, *J. Am. Chem. Soc.*, 2012, **134**, 2512.